Electronic Supplementary Material (ESI) for ChemComm.

Acid/base-controllable Fluorescent Molecular Switches Based on Cryptands and *N*-Heteroaromatics

Ming Cheng,[a] Jing Zhang,[a] Xintong Ren,[a] Shuwen Guo,[a] Tangxin Xiao,[b] Xiao-Yu Hu,[a] Juli Jiang,*[a] and Leyong Wang*[a,b]

a. Key Laboratory of Mesoscopic Chemistry of MOE, School of Chemistry and Chemical Engineering, Nanjing University, Nanjing 210023(China).
b. Institute for Natural & Synthetic Organic Chemistry, Changzhou University, Changzhou, 213164, China.
E-mail: jjl@nju.edu.cn, lywang@nju.edu.cn

SUPPORTING INFORMATION

Table of Contents

1. Materials and methods

All reactions were performed in open atmosphere unless otherwise stated. All reagents, unless otherwise indicated, were obtained from commercial sources. Anhydrous CH_2Cl_2 was obtained by distillation from CaH_2 under N_2 atmosphere. Melting points (M.p.) were determined using a Focus X-4 apparatus and were not corrected. All yields were given as isolated yields. NMR spectra were recorded on a Bruker DPX 400 MHz or 500 MHz spectrometer with internal standard tetramethylsilane (TMS) and solvent signals as internal references, and the chemical shifts (δ) were expressed in ppm and J values were given in Hz. 2D ROESY experiments were performed on a Bruker DPX 400 MHz spectrometer. High-resolution electrospray ionization mass spectra (HR-ESI-MS) were recorded on an Agilent 6540Q-TOF LC-MS equipped with an electrospray ionization (ESI) probe operating in positive-ion mode with direct infusion.

2. Experimental procedures.

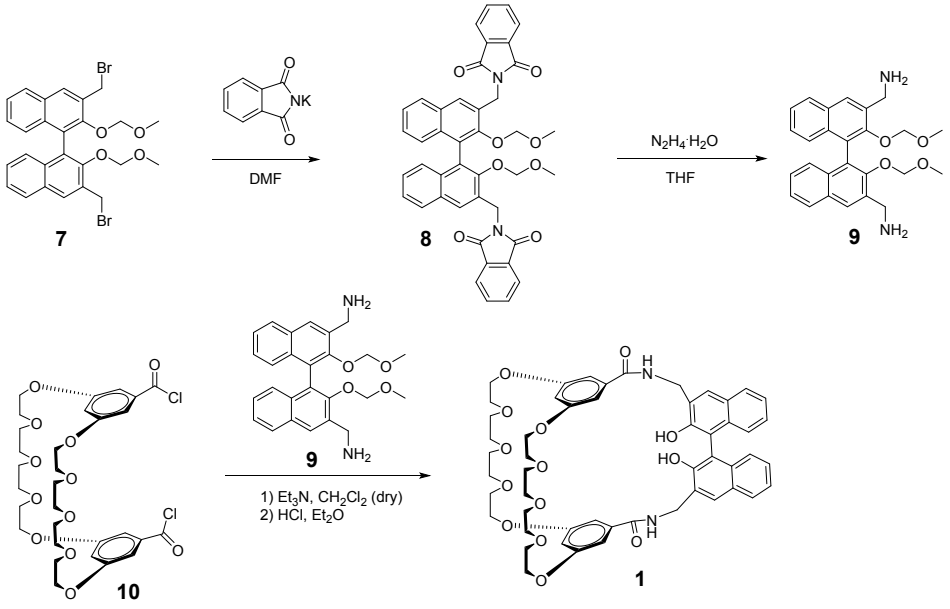

Scheme S1. Synthesis of cryptand **1**.

Compound 8: A mixture of **7**[1] (0.55 g, 0.98 mmol) and compound Potassium phthalimide (0.36 g, 1.96 mmol) in anhydrous DMF was stirred for 24 h. The reaction mixture was filtered. The filtrate was removed in vacuum and the residue was dissolved in CH_2Cl_2. The organic phase was washed with water, dried over anhydrous Na_2SO_4 and concentrated under vacuum. The residue was

purified by silica-gel column chromatography using (PE/EA = 4:1, *v/v*) to afford **8** (4.07 g, 60.0%) as a yellow solid. M.p.113-115 ^{o}C ; The ^{1}H NMR & ^{13}C NMR spectra of **8** are shown in Fig. S1-S2. ^{1}H NMR (400 MHz, $CDCl_3$, 298K) δ (ppm): 7.96-7.94 (m, 4H), 7.81-7.79(m, 4H), 7.75 (d, J = 8.1 Hz, 2H), 7.64 (s, 2H), 7.37-7.33 (m, 2H), 7.23 (d, J = 8.1 Hz, 2H), 7.17 (d, J = 8.38 Hz, 2H), 5.33-5.20 (m, 4H), 4.67-4.64 (m, 4H), 2.99 (s, 6H).; ^{13}C NMR (100 MHz, $CDCl_3$, 298 K) δ (ppm): 168.3, 152.0, 134.2, 133.6, 132.2, 130.6, 129.8, 127.9, 126.9, 126.6, 126.0, 125.3, 125.2, 123.6, 99.3, 57.0, 37.6.; HR-MS (ESI): calcd. for [**8** + Na]$^{+}$: 775.2051, found m/z = 715.2049.

Compound 9: **8** (1.00 g, 1.44 mmol) in tetrahydrofuran was heated to reflux at 80 °C. Then $N_2H_4 \cdot H_2O$ (0.70 mL, 14.45 mmol) was added. The reaction system was refluxed for 12 h. After the solution was cooled to 25 ºC, the solvent was evaporated under reduced pressure. The residue was dissolved in CH_2Cl_2 (30 mL), and the organic phase was washed with water (2 × 30 mL), dried over anhydrous Na_2SO_4 and concentrated under vacuum. The residue was purified by silica-gel column chromatography (CH_2Cl_2/CH_3OH = 50:1, *v/v*) to afford **9** as a yellow oil (0.45 g, 1.56 mmol, 72%). The ^{1}H & ^{13}C NMR spectra of **9** are shown in Figure S4-S5. ^{1}H NMR (400 MHz, CD_3CN, 298K) δ (ppm): 8.06 (s, 2H), 7.93 (d, J = 8.2 Hz, 2H), 7.41 (t, J = 7.1 Hz, 2H), 7.21 (dd, J = 11.2, 4.1 Hz, 2H), 7.04 (d, J = 8.4 Hz, 2H), 4.52 (dd, J = 35.0, 5.6 Hz, 4H), 4.05 (q, J = 15.2 Hz, 4H), 2.88 (s, 6H), 2.09 (b, 4H); ^{13}C NMR ($CDCl_3$, 75 MHz, 298K) δ (ppm): 153.1, 136.9, 133.5, 131.0, 128.1, 127.9, 126.5, 126.0, 125.3, 125.2, 99.3, 57.0, 42.9, 30.4, 29.8, 29.8, 22.8, 14.2.; HR-MS (ESI): Calcd. for [**8** + H]$^{+}$: 433.2122; Found: 433.2119.

Compound 1: a solution of **10**[2] (0.50 g, 0.76 mmol) in dry CH_2Cl_2 (50 mL) was added slowly to a solution of **9** (0.33 g, .076 mmol) and Et_3N (2.00 mL) in dry CH_2Cl_2 (300 mL) under argon gas protection. After complete addition, the mixture was stirred at room temperature for 3 days. After the solvent was removed under vacuum, dissolved in dichloromethane (30 mL), the organic phase was washed with water (2 × 30 mL). The organic phase condensed in vacuum to give a white solid. The solid was re-dissolved with the solution of HCl in ethanol. The solution was refluxed for 2 hours, remove the organic solvents under vacuum. The residue was dissolved in CH_2Cl_2 (30 mL), and the organic phase was washed with water (2 × 30 mL), dried over anhydrous Na_2SO_4 and concentrated under vacuum. The residue was purified by silica-gel column chromatography using (CH_2Cl_2/CH_3OH = 60:1, *v/v*) to afford **1** (0.14 g, 20%) as a white solid. M.p.133-135 ^{o}C ; The ^{1}H

NMR & ^{13}C NMR spectra of **1** are shown in Fig. S7-S8. ^{1}H NMR (400 MHz, $CDCl_3$, 298K) δ (ppm): 7.98 (s, 2H), 7.85 (d, J = 8.1 Hz, 2H), 7.36-7.28 (m, 6H), 7.17 (d, J = 8.2 Hz, 2H), 6.84 (s, 4H), 6.54 (s, 2H), 4.86-4.77 (m, 4H), 4.04-3.94 (m, 8H), 3.77-3.58 (m, 24H).; ^{13}C NMR (100 MHz, CD_3CN, 298 K) δ (ppm): 165.9, 159.7, 159.6, 148.9, 145.7, 144.4, 138.6, 138.2, 114.4, 111.6, 107.6, 107.5, 107.5, 107.2, 102.1, 100.3, 100.2, 71.5, 71.0, 70.1, 69.9, 68.9, 67.3, 67.2, 46.7, 44.2, 25.5.; HR-MS (ESI): calcd. for $[\mathbf{1} + H]^+$: 933.3804, found m/z = 933.3791.

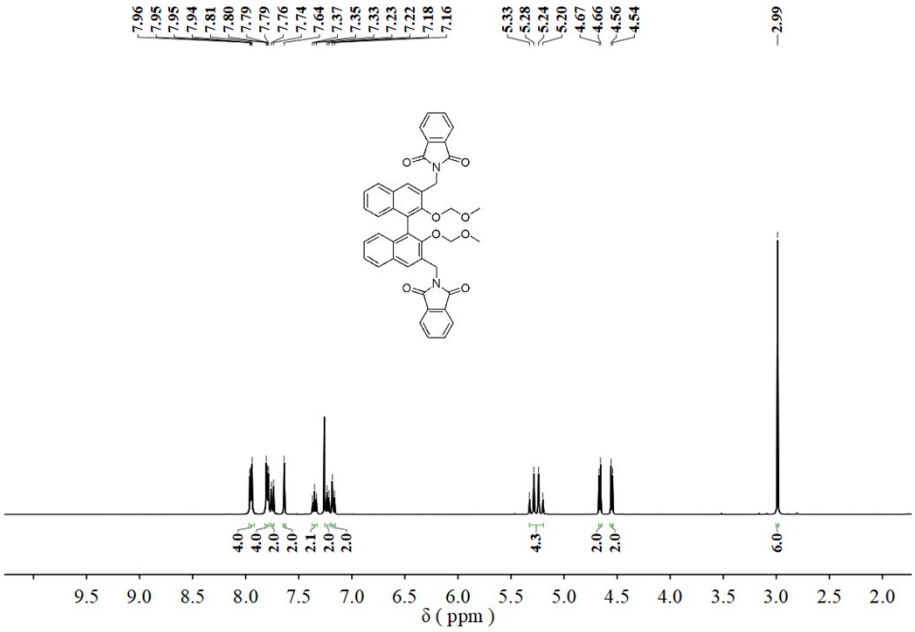

Fig. S1 ^{1}H NMR spectrum (400 MHz, $CDCl_3$, 298 K) of compound **8**.

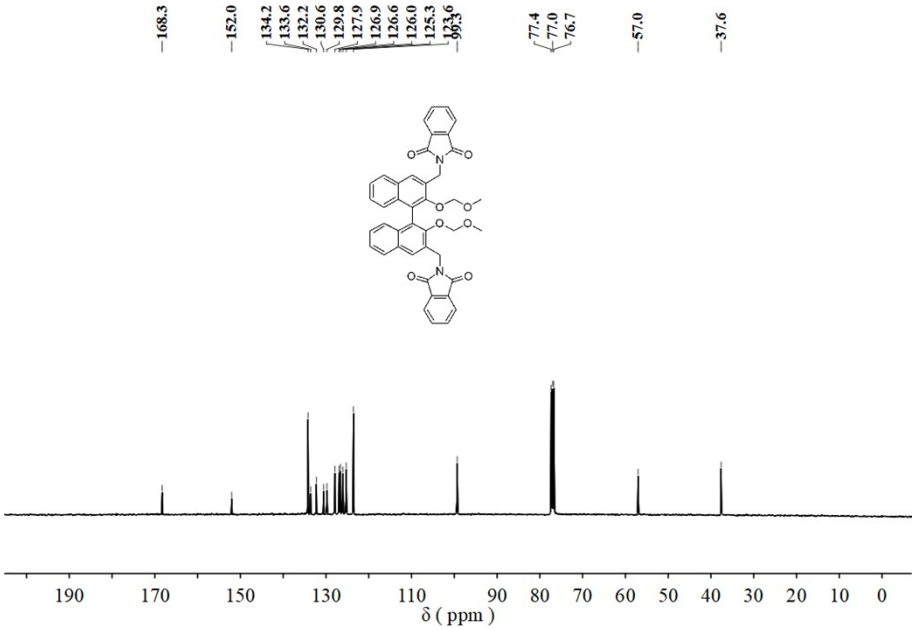

Fig. S2 ^{13}C NMR spectrum (100 MHz, $CDCl_3$, 298 K) of compound **8**.

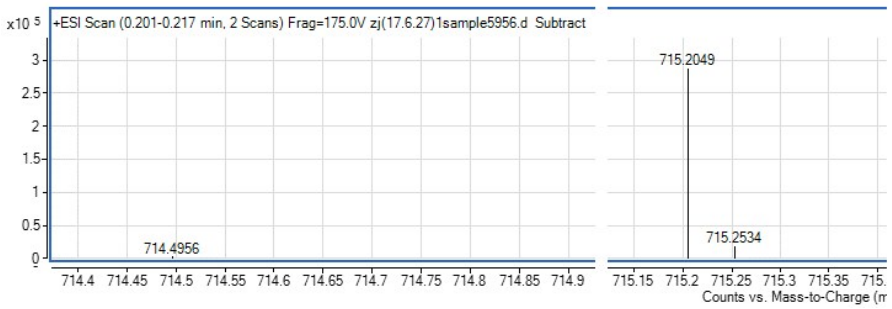

Fig. S3 HR-ESI-MS of compound **8**.

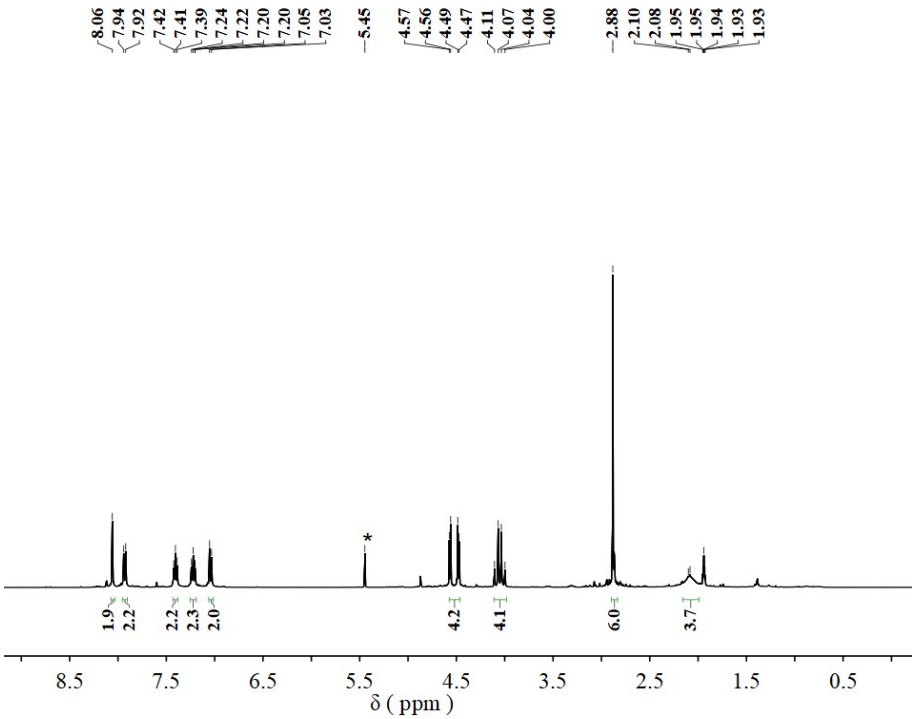

Fig. S4 ^{1}H NMR spectrum (400 MHz, CD_3CN, 298 K) of compound **9**. (*signals of CH_2Cl_2).

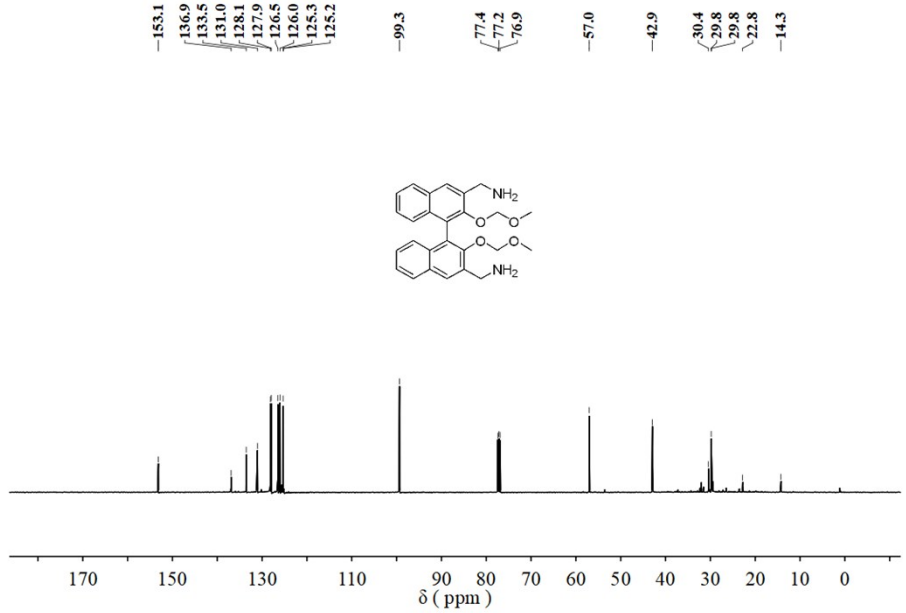

Fig. S5 ^{13}C NMR spectrum (100 MHz, $CDCl_3$, 298 K) of compound **9**.

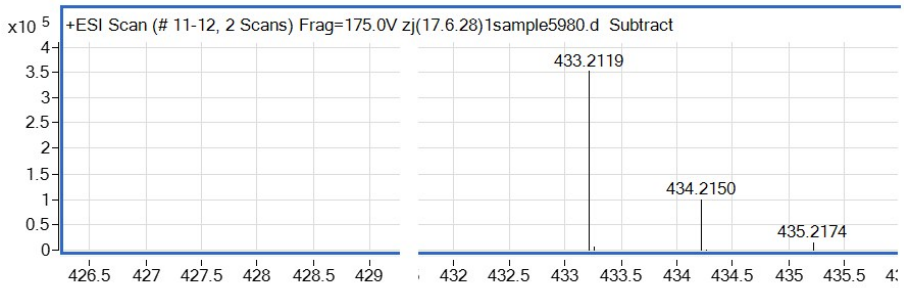

Fig. S6 HR-ESI-MS of compound **9**.

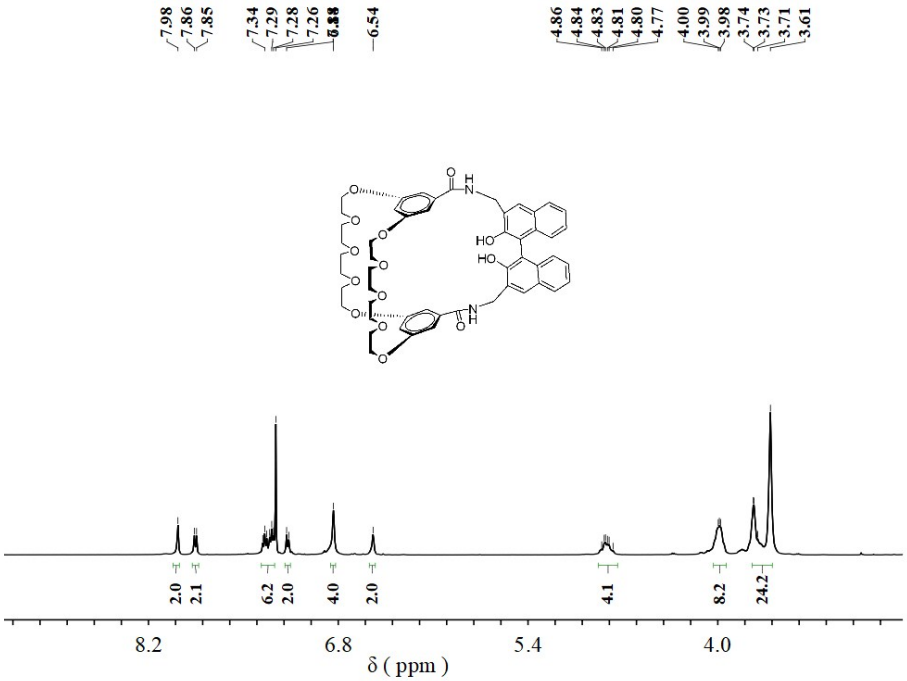

Fig. S7 ^{1}H NMR spectrum (400 MHz, $CDCl_3$, 298 K) of compound **1**.

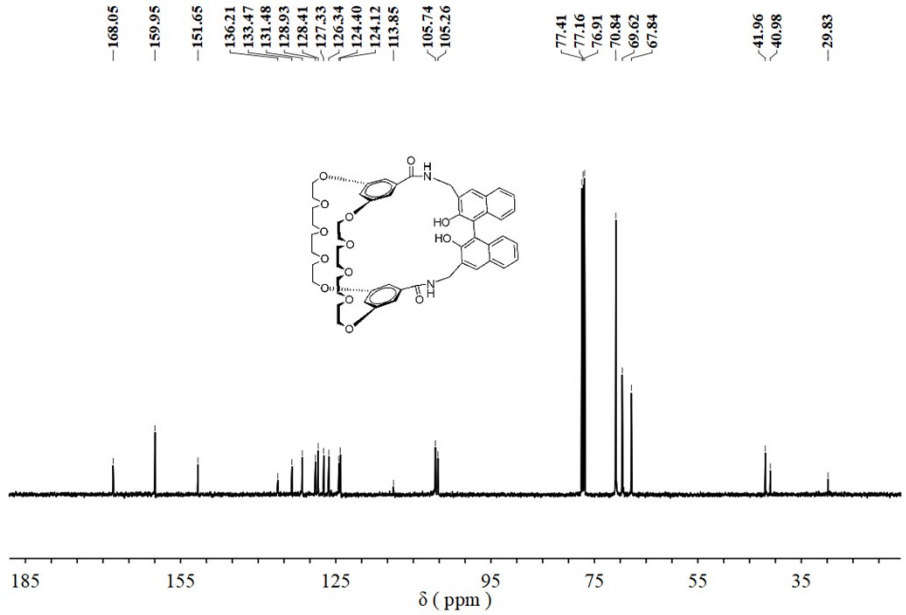

Fig. S8 ^{13}C NMR spectrum (100 MHz, $CDCl_3$, 298 K) of compound **1**.

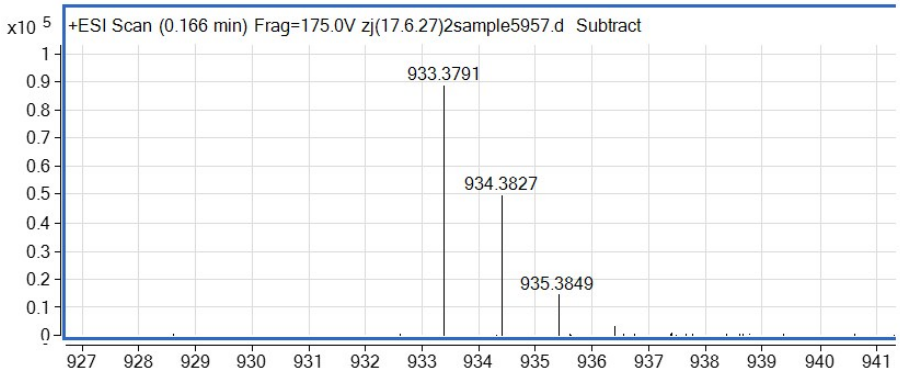

Fig. S9 HR-ESI-MS of compound **1**.

3. Association constants and Job plots.

3.1 ^{1}HNMR spectra between cryptand 1, cryptand 2 and four guests in acid/base conditions

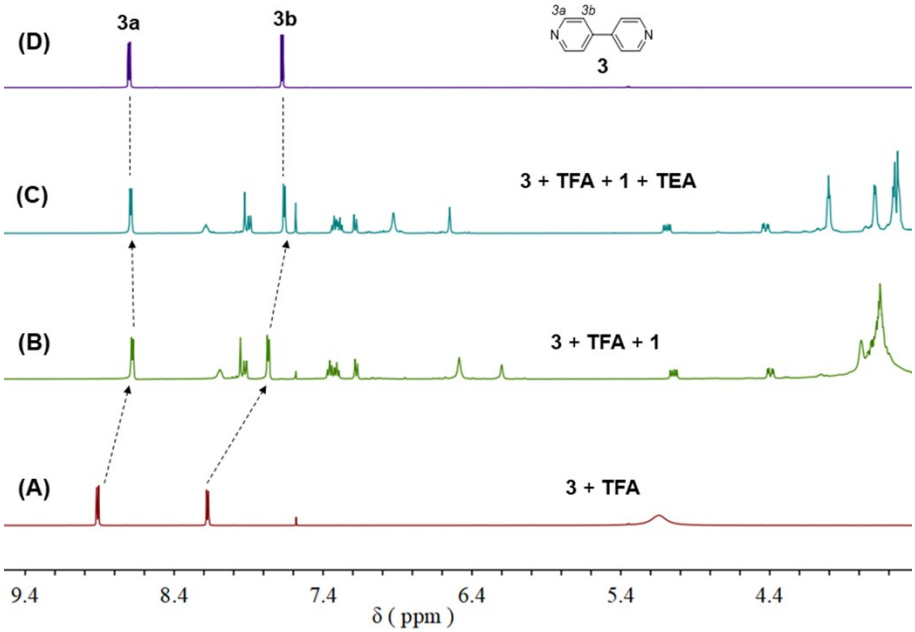

Fig. S10 Partial ^{1}HNMR spectra (500MHz, CD_3CN, 298 K): (A) 5.00 mM **3** + 4.0 equiv. **TFA**; (B) 5.00 mM **3** + 4.0 equiv. **TFA** + 5.00 mM **1**; (C) 5.00 mM **3** + 4.0 equiv. **TFA** + 5.00 mM **1** + 6.0 equiv. **TEA**; (D) 5.00 mM **3**.

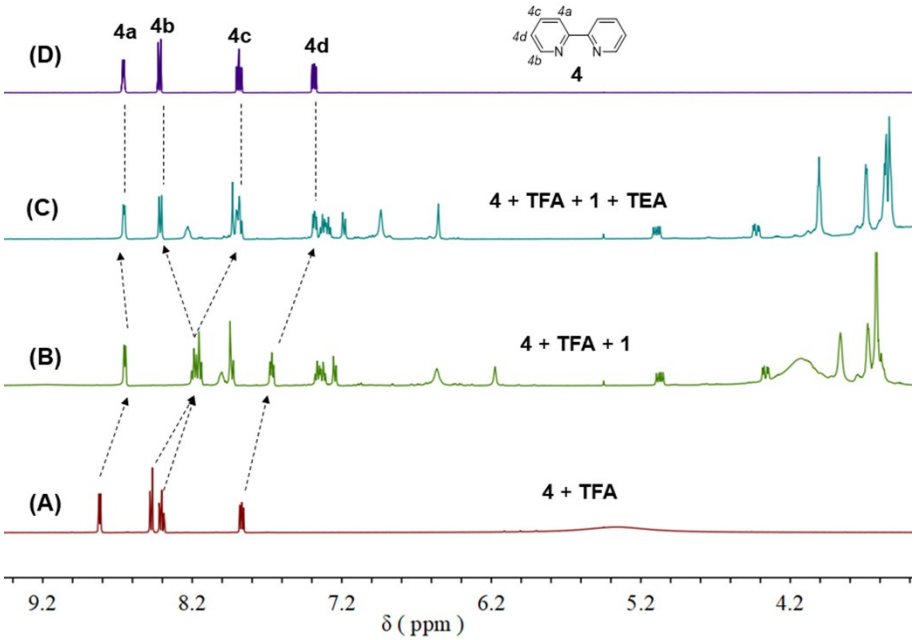

Fig. S11 Partial ^{1}HNMR spectra (500MHz, CD_3CN, 298 K): (A) 5.00 mM **4** + 4.0 equiv. **TFA**; (B) 5.00 mM **4** + 4.0 equiv. **TFA** + 5.00 mM **1**; (C) 5.00 mM **4** + 4.0 equiv. **TFA** + 5.00 mM **1** + 6.0 equiv. **TEA**; (D) 5.00 mM **4**.

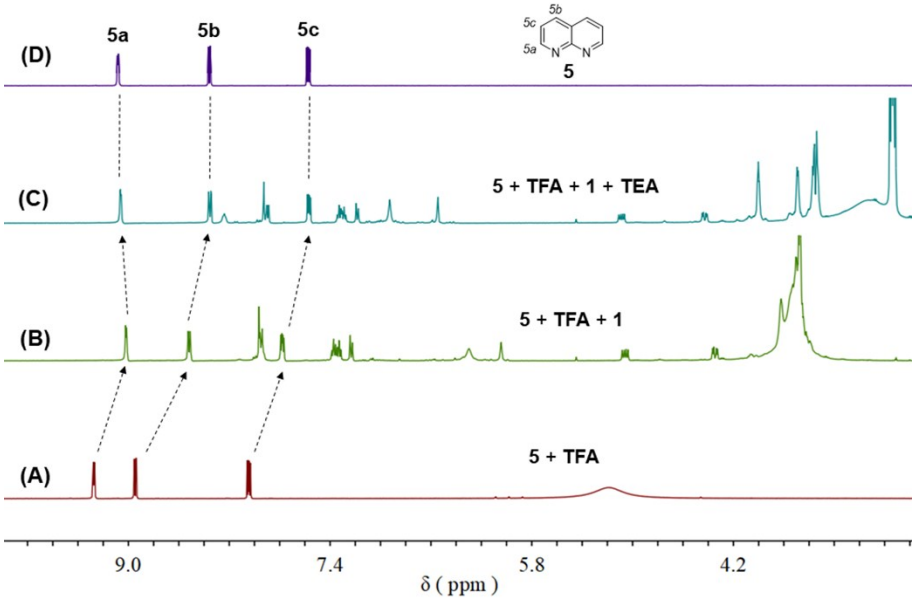

Fig. S12 Partial ^{1}HNMR spectra (500MHz, CD_3CN, 298 K): (A) 5.00 mM **5** + 4.0 equiv. **TFA**; (B) 5.00 mM **5** + 4.0 equiv. **TFA** + 5.00 mM **1**; (C) 5.00 mM **5** + 4.0 equiv. **TFA** + 5.00 mM **1** + 6.0 equiv. **TEA**; (D) 5.00 mM **5**.

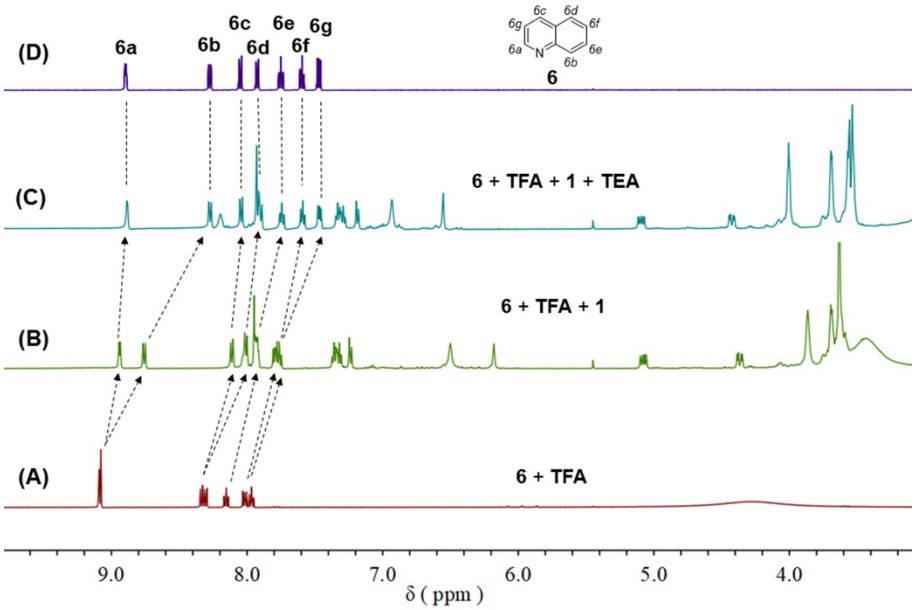

Fig. S13 Partial ^{1}HNMR spectra (500MHz, CD_3CN, 298 K): (A) 5.00 mM **6** + 2.0 equiv. **TFA**; (B) 5.00 mM **6** + 2.0 equiv. **TFA** + 5.00 mM **1**; (C) 5.00 mM **6** + 2.0 equiv. **TFA** + 5.00 mM **1** + 3.0 equiv. **TEA**; (D) 5.00 mM **6**.

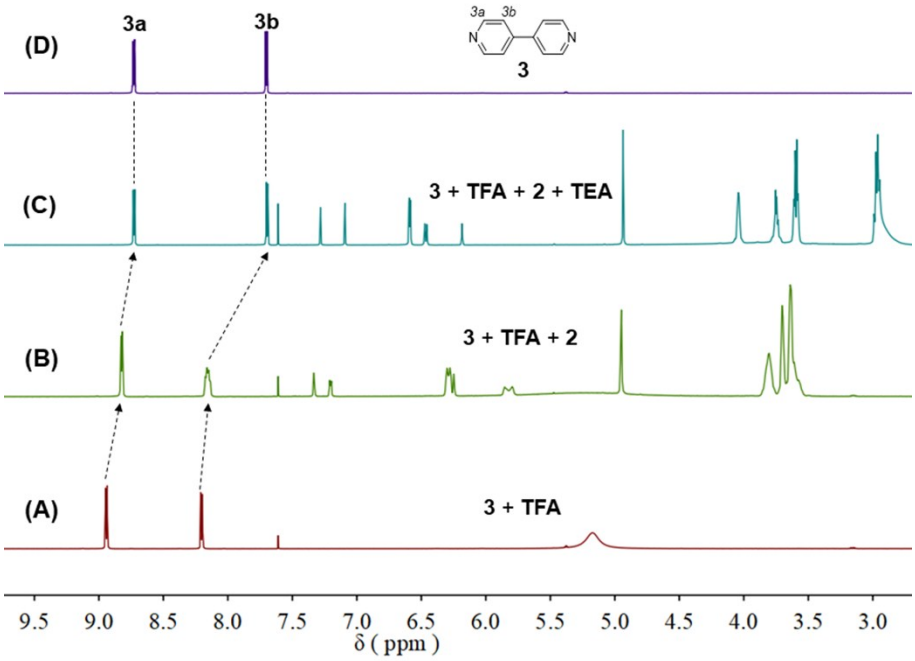

Fig. S14 Partial ^{1}HNMR spectra (500MHz, CD_3CN, 298 K): (A) 5.00 mM **3** + 4.0 equiv. **TFA**; (B) 5.00 mM **3** + 4.0 equiv. **TFA** + 5.00 mM **2**; (C) 5.00 mM **3** + 4.0 equiv. **TFA** + 5.00 mM **2** + 6.0 equiv. **TEA**; (D) 5.00 mM **3**.

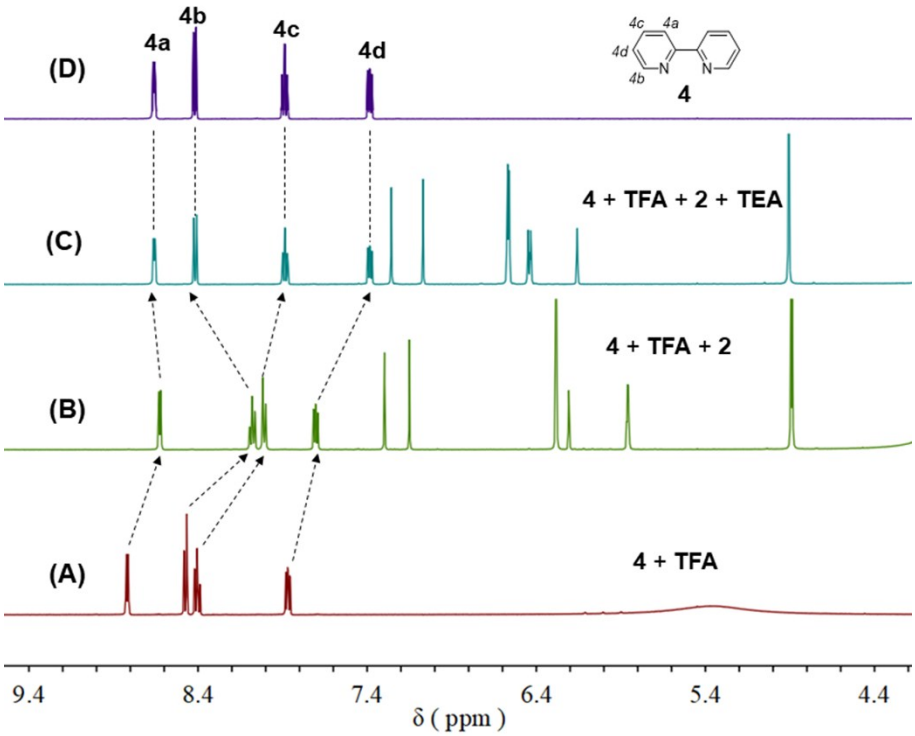

Fig. S15 Partial ^{1}HNMR spectra (500MHz, CD_3CN, 298 K): (A) 5.00 mM **4** + 4.0 equiv. **TFA**; (B) 5.00 mM **4** + 4.0 equiv. **TFA** + 5.00 mM **2**; (C) 5.00 mM **4** + 4.0 equiv. **TFA** + 5.00 mM **2** + 6.0 equiv. **TEA**; (D) 5.00 mM **4**.

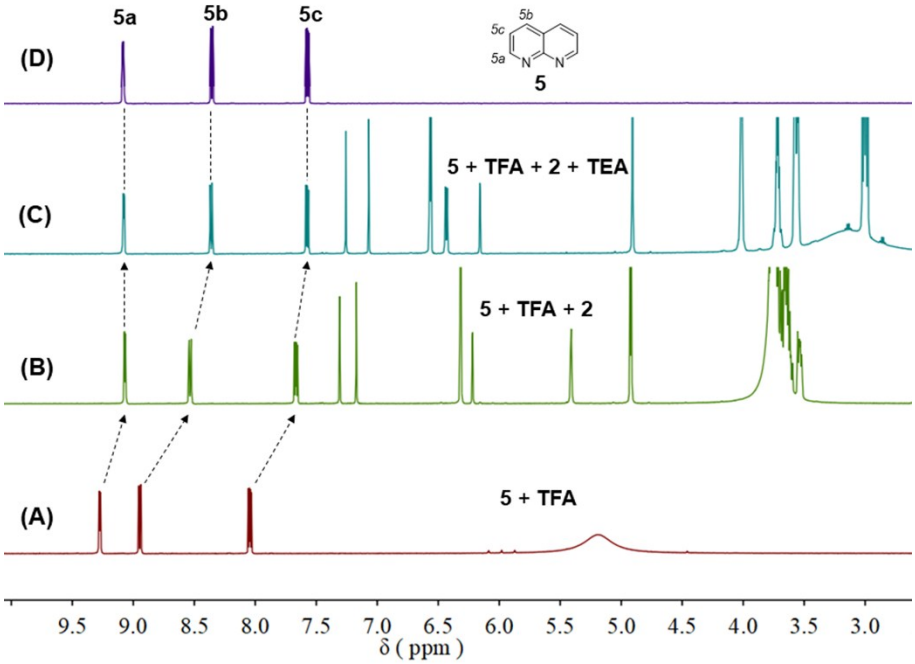

Fig. S16 Partial ^{1}HNMR spectra (500MHz, CD_3CN, 298 K): (A) 5.00 mM **5** + 4.0 equiv. **TFA**; (B) 5.00 mM **5** + 4.0 equiv. **TFA** + 5.00 mM **2**; (C) 5.00 mM **5** + 4.0 equiv. **TFA** + 5.00 mM **2** + 6.0 equiv. **TEA**; (D) 5.00 mM **5**.

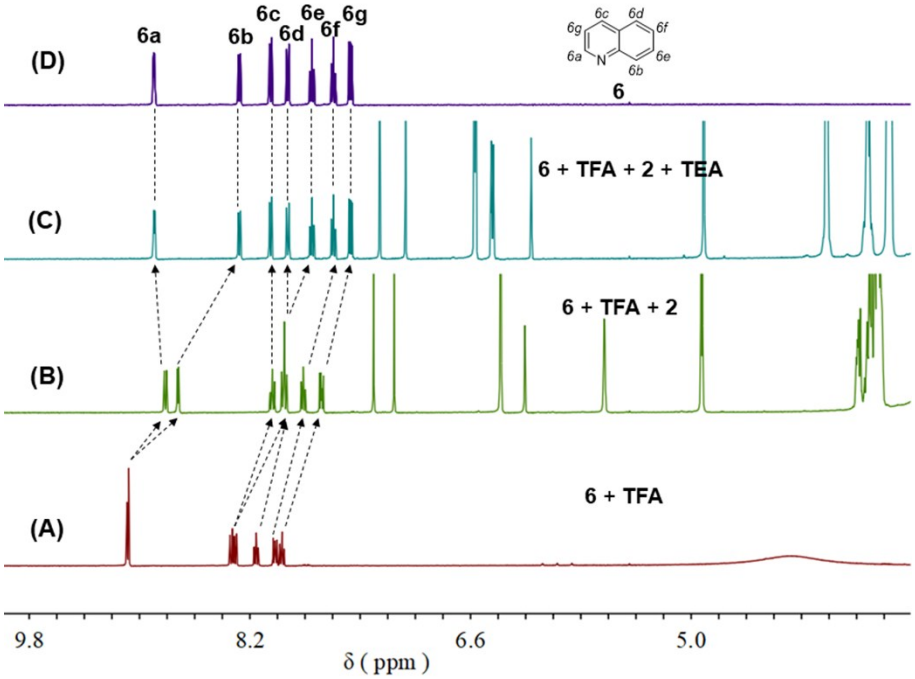

Fig. S17 Partial [1]HNMR spectra (500MHz, CD_3CN, 298 K): (A) 5.00 mM **6** + 2.0 equiv. **TFA**; (B) 5.00 mM **6** + 2.0 equiv. **TFA** + 5.00 mM **2**; (C) 5.00 mM **6** + 2.0 equiv. **TFA** + 5.00 mM **2** + 3.0 equiv. **TEA**; (D) 5.00 mM **6**.

3.2 Job plot for cryptand 1, cryptand 2 with four guests.

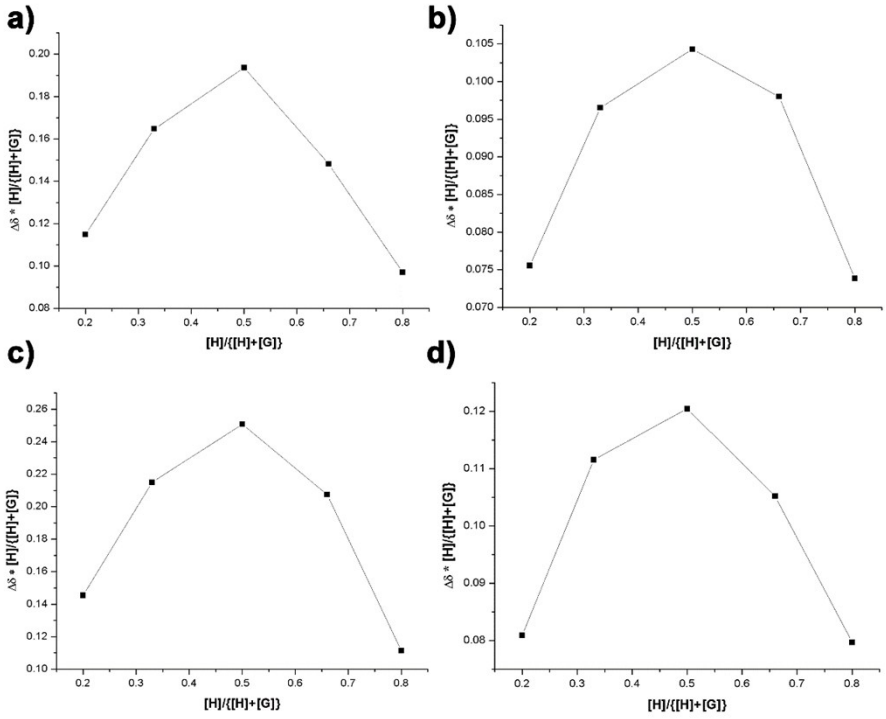

Fig. S18 The Job Plot (NMR titrations) for the complexation of (a) **1** with **3'** ; (b) **1** with **4'**; (c) **1** with **5'**; (d) **1** with **6'**; in CD_3CN at 298 K. ([H] + [G] = 8 mM).

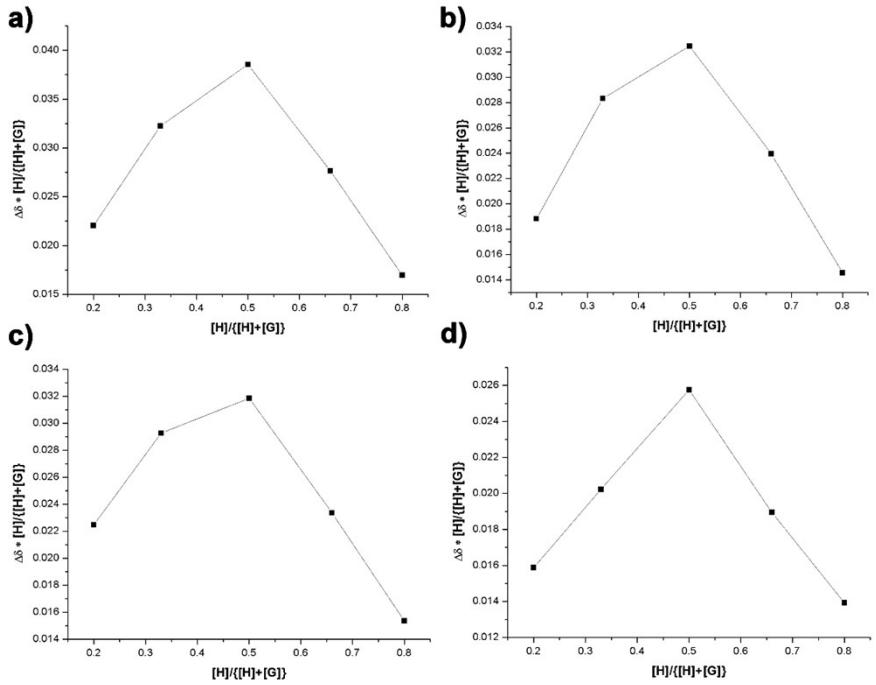

Fig. S19 The Job Plot (NMR titrations) for the complexation of (a) **2** with **3'**; (b) **2** with **4'**; (c) **2** with **5'**; (d) **H2** with **6'**; in CD_3CN at 298 K. ([H] + [G] = 8 mM).

3.3 Determination of the association constants

^{1}H NMR titrations were performed with a constant concentration of host (2.00 mM) and varying concentrations of guest in the range of 1.0 – 40.0 mM. Using a nonlinear curve-fitting method, the association constant was obtained for each host-guest combination from the following equation:

$$\Delta\delta = (\Delta\delta_\infty/[H]_0)\ (0.5[G]_0 + 0.5([H]_0 + 1/K_a) - (0.5\ (\ [G]_0^2 + (2[G]_0(1/K_a - [H]_0)) + (1/K_a + [H]_0)^2)^{0.5})) \quad \text{(Eq. S1)}$$

Where $\Delta\delta$ is the chemical shift change of H_{1a} on cryptand **1** (H_{2d} on crypand **2**) at $[H]_0$, $\Delta\delta_\infty$ is the chemical shift change of H_a when the guest is completely complexed, $[G]_0$ is the fixed initial concentration of the guest, and $[H]_0$ is the initial concentration of the host.

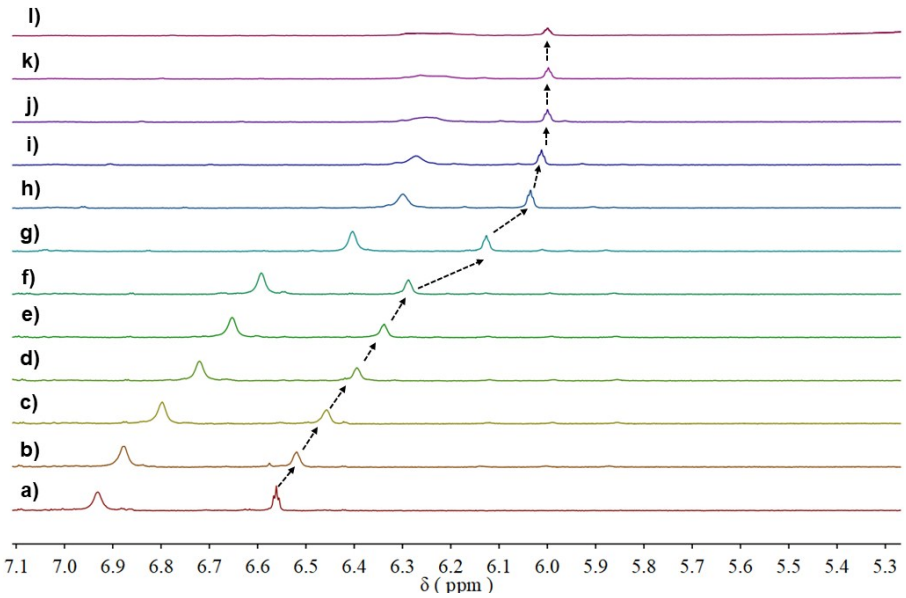

Fig. S20 Partial ^{1}H NMR spectrum changes (400 MHz, CD_3CN, 298 K) of **1** (host, 2.00 mM) upon addition of **3'** (guest): (a) 0.00, (b) 0.40, (c) 0.80, (d) 1.20, (e) 1.60, (f) 2.00, (g) 4.00, (h) 8.00, (i) 12.00, (j) 20.00, (k) 30.00, (l) 40.00 mM.

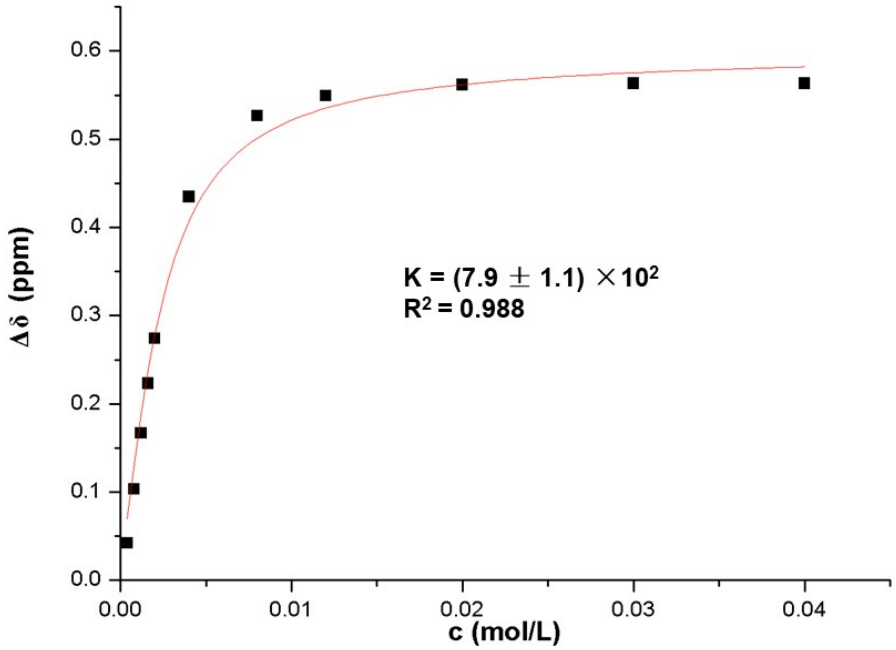

Fig. S21 The non-linear curve-fitting (NMR titrations) for the complexation of **1** (host) with **3'** (guest) in CD_3CN at 298 K. Using the signal of **1** at δ 6.5612 as the reference. The association constant (*K*a) of **1⊃3'** in CD_3CN was estimated to be about (7.90 ± 1.10) ×10^2.

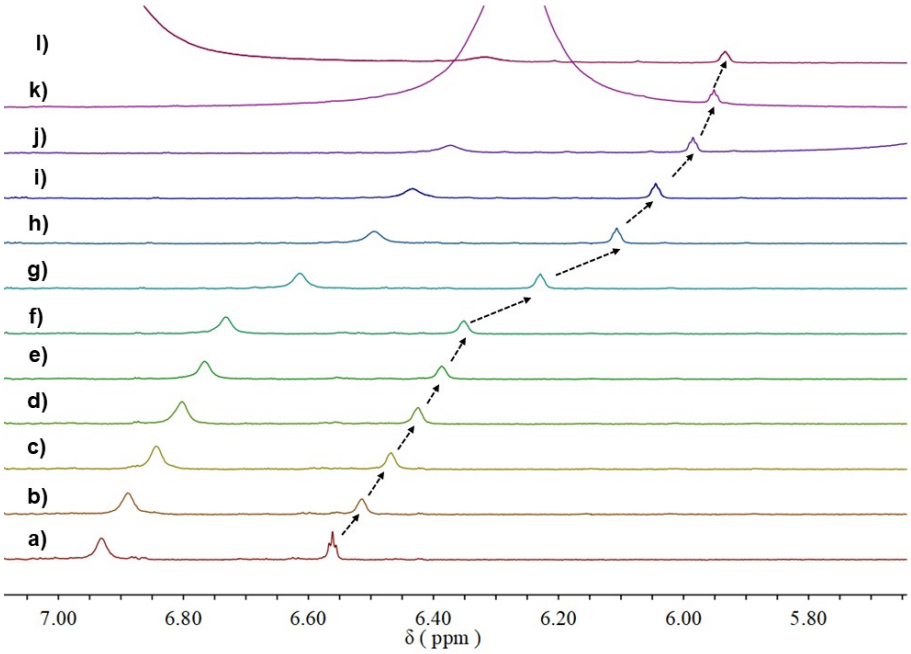

Fig. S22 Partial ^{1}H NMR spectrum changes (400 MHz, CD_3CN, 298 K) of **1** (host, 2.00 mM) upon addition of **4'** (guest): (a) 0.00, (b) 0.40, (c) 0.80, (d) 1.20, (e) 1.60, (f) 2.00, (g) 4.00, (h) 8.00, (i) 12.00, (j) 20.00, (k) 30.00, (l) 40.00 mM.

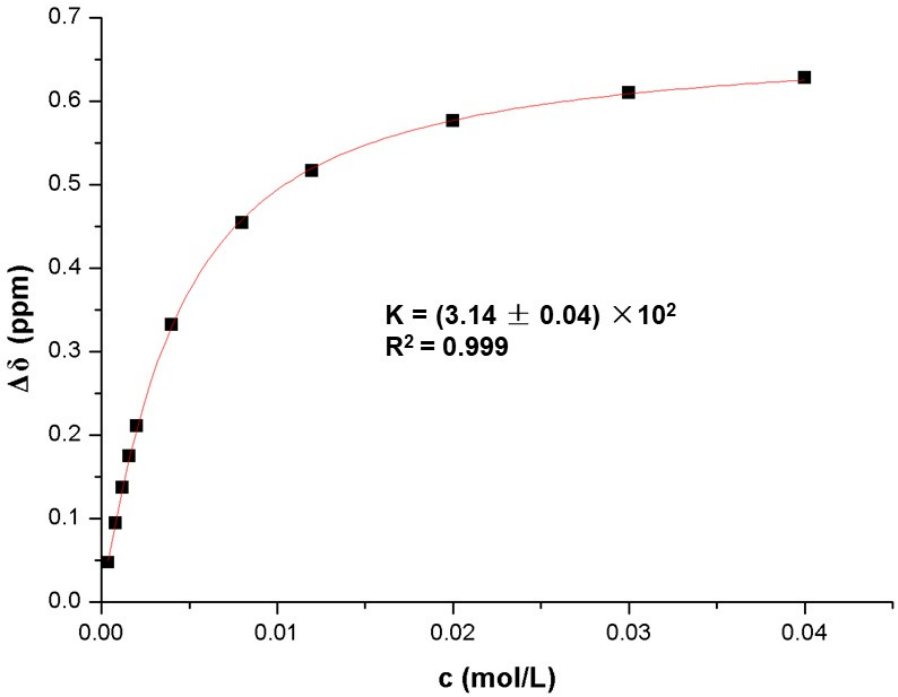

Fig. S23 The non-linear curve-fitting (NMR titrations) for the complexation of **1** (host) with **4'** (guest) in CD_3CN at 298 K. Using the signal of **1** at δ 6.5612 as the reference. The association constant (*K*a) of **1⊃4'** in CD_3CN was estimated to be about $(3.14 \pm 0.04) \times 10^2$.

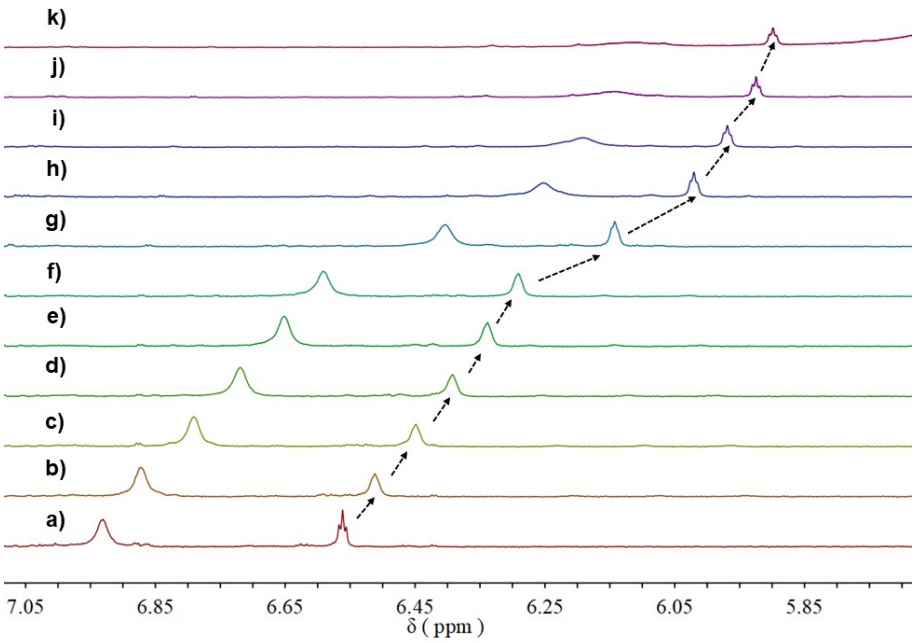

Fig. S24 Partial ^{1}H NMR spectrum changes (400 MHz, CD_3CN, 298 K) of **1** (host, 2.00 mM) upon addition of **5'** (guest): (a) 0.00, (b) 0.40, (c) 0.80, (d) 1.20, (e) 1.60, (f) 2.00, (g) 4.00, (h) 8.00, (i) 12.00, (j) 20.00, (k) 30.00 mM.

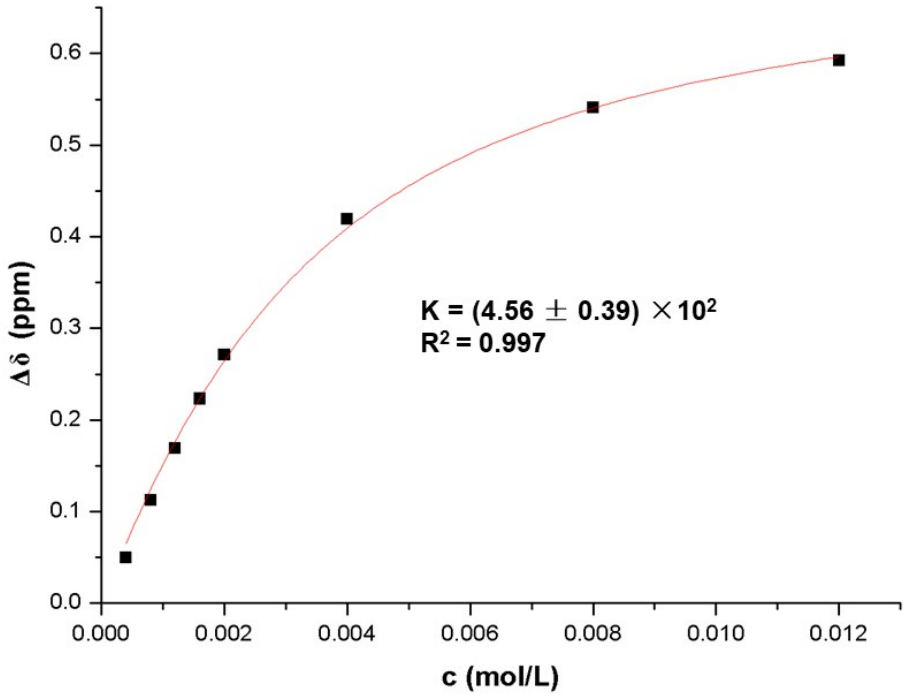

Fig. S25 The non-linear curve-fitting (NMR titrations) for the complexation of **1** (host) with **5'** (guest) in CD_3CN at 298 K. Using the signal of **1** at δ 6.5612 as the reference. The association constant (*K*a) of **1⊃5'** in CD_3CN was estimated to be about $(4.56 \pm 0.39) \times 10^2$.

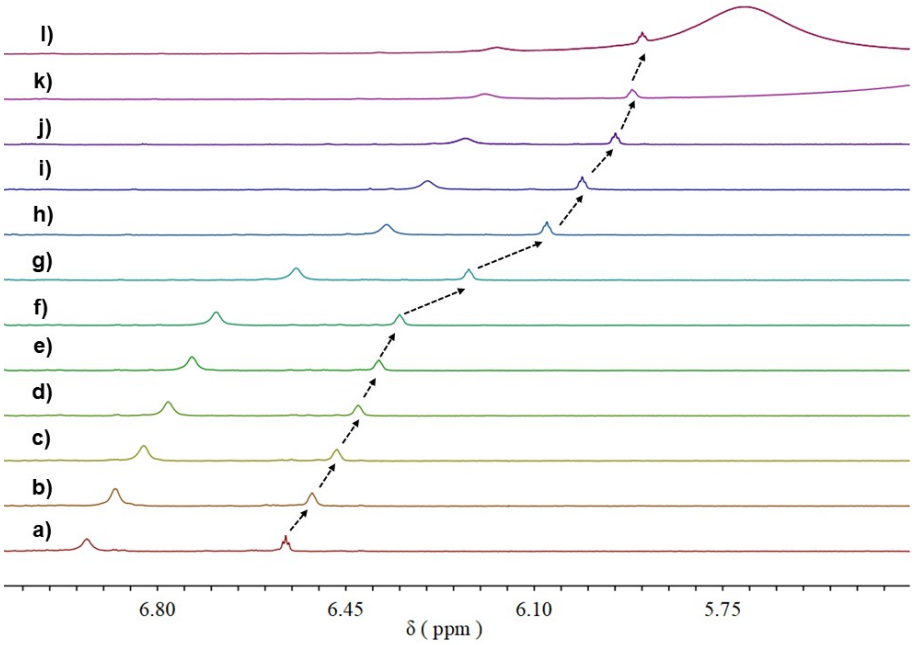

Fig. S26 Partial ^{1}H NMR spectrum changes (400 MHz, CD_3CN, 298 K) of **1** (host, 2.00 mM) upon addition of **6'** (guest): (a) 0.00, (b) 0.40, (c) 0.80, (d) 1.20, (e) 1.60, (f) 2.00, (g) 4.00, (h) 8.00, (i) 12.00, (j) 20.00, (k) 30.00, (l) 40.00 mM.

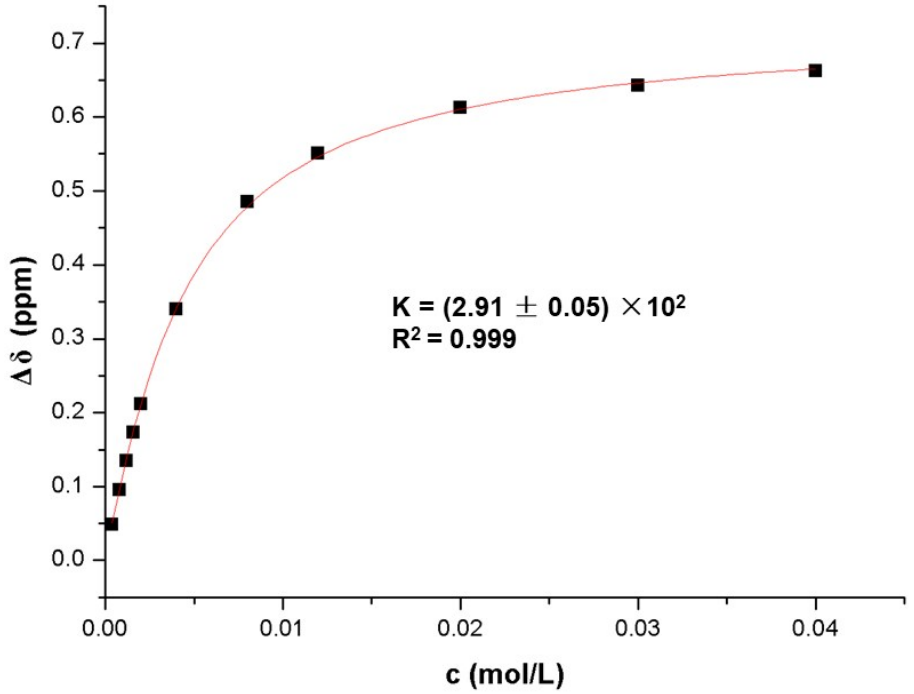

Fig. S27 The non-linear curve-fitting (NMR titrations) for the complexation of **1** (host) with **6'** (guest) in CD_3CN at 298 K. Using the signal of **1** at δ 6.5612 as the reference. The association constant (*K*a) of **1⊃6'** in CD_3CN was estimated to be about (2.91 ± 0.05) ×10^2.

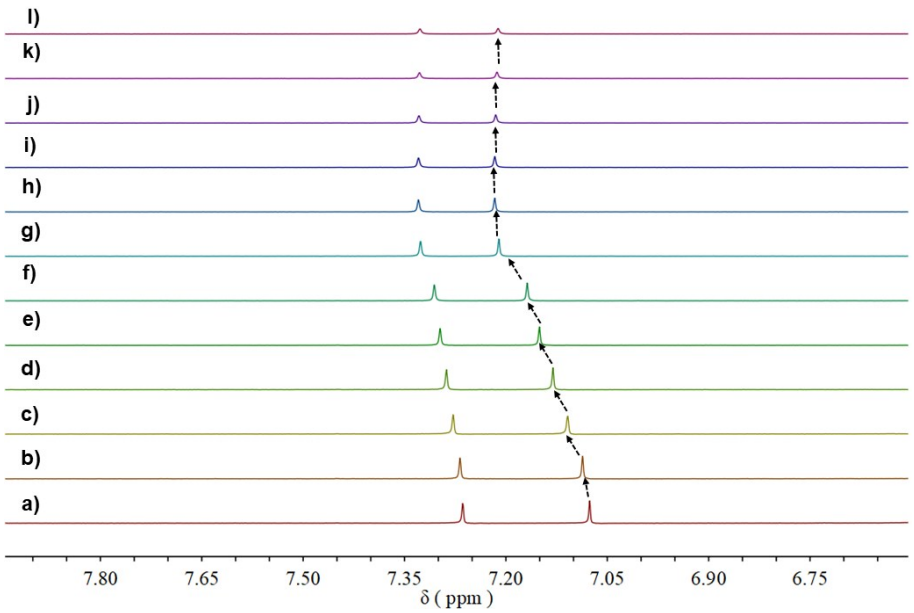

Fig. S28 Partial ^{1}H NMR spectrum changes (500 MHz, CD_3CN, 298 K) of **2** (host, 2.00 mM) upon addition of **3'** (guest): (a) 0.00, (b) 0.40, (c) 0.80, (d) 1.20, (e) 1.60, (f) 2.00, (g) 4.00, (h) 8.00, (i) 12.00, (j) 20.00, (k) 30.00, (l) 40.00 mM.

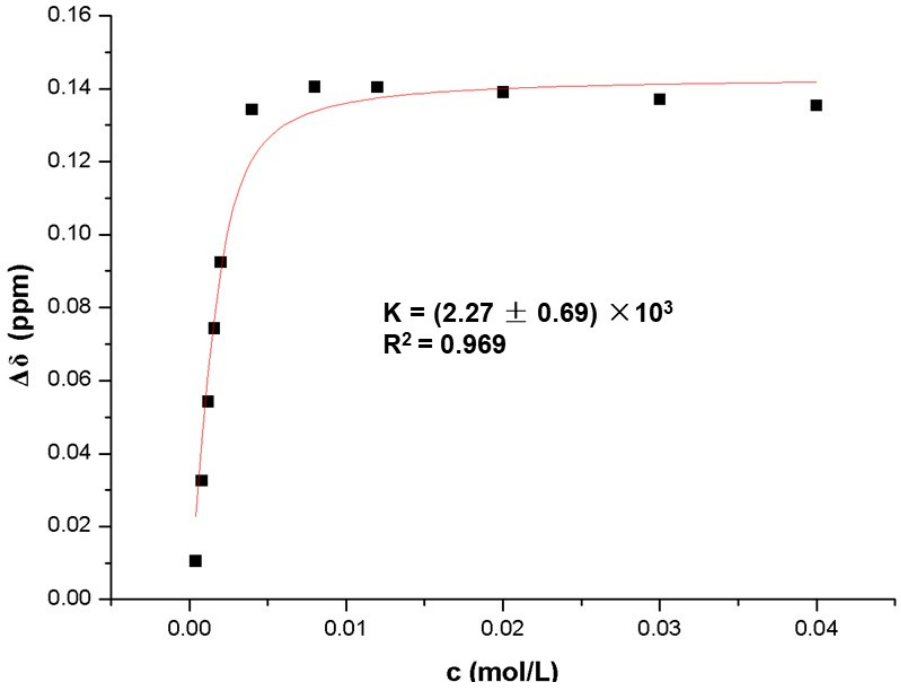

Fig. S29 The non-linear curve-fitting (NMR titrations) for the complexation of **2** (host) with **3'** (guest) in CD_3CN at 298 K. Using the signal of **2** at δ 7.0761 as the reference. The association constant (*K*a) of **2⊃3'** in CD_3CN was estimated to be about (2.27 ± 0.69) ×10^3.

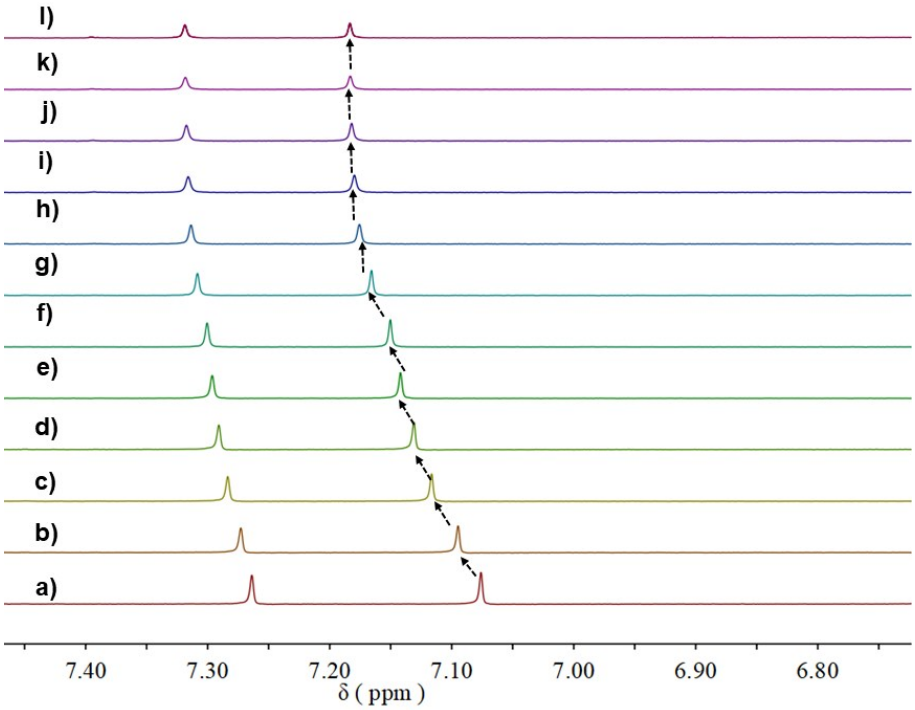

Fig. S30 Partial ^{1}H NMR spectrum changes (500 MHz, CD_3CN, 298 K) of **2** (host, 2.00 mM) upon addition of **4'** (guest): (a) 0.00, (b) 0.40, (c) 0.80, (d) 1.20, (e) 1.60, (f) 2.00, (g) 4.00, (h) 8.00, (i) 12.00, (j) 20.00, (k) 30.00, (l) 40.00 mM.

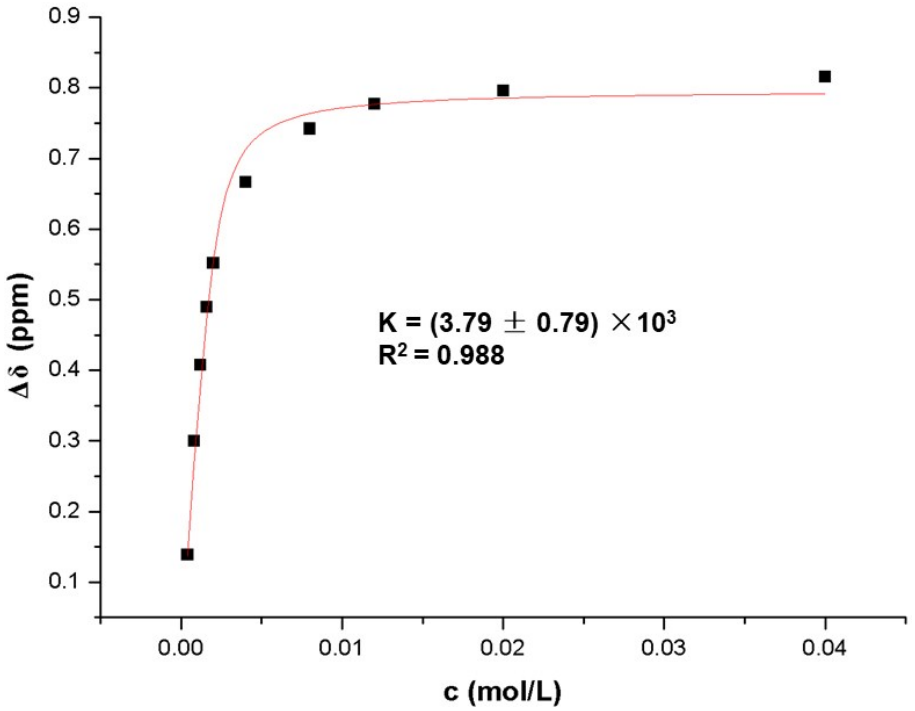

Fig. S31 The non-linear curve-fitting (NMR titrations) for the complexation of **2** (host) with **4'** (guest) in CD_3CN at 298 K. Using the signal of **2** at δ 7.0761 as the reference. The association constant (*K*a) of **2⊃4'** in CD_3CN was estimated to be about (3.79 ± 0.79) ×10^3.

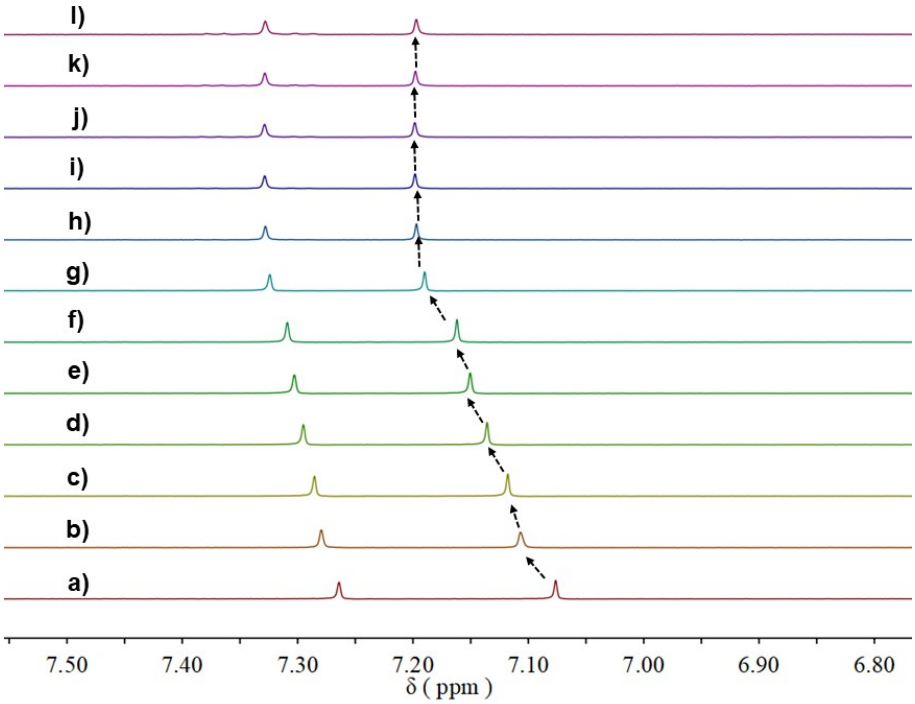

Fig. S32 Partial ^{1}H NMR spectrum changes (500 MHz, CD_3CN, 298 K) of **2** (host, 2.00 mM) upon addition of **5'** (guest): (a) 0.00, (b) 0.40, (c) 0.80, (d) 1.20, (e) 1.60, (f) 2.00, (g) 4.00, (h) 8.00, (i) 12.00, (j) 20.00, (k) 30.00, (l) 40.00 mM.

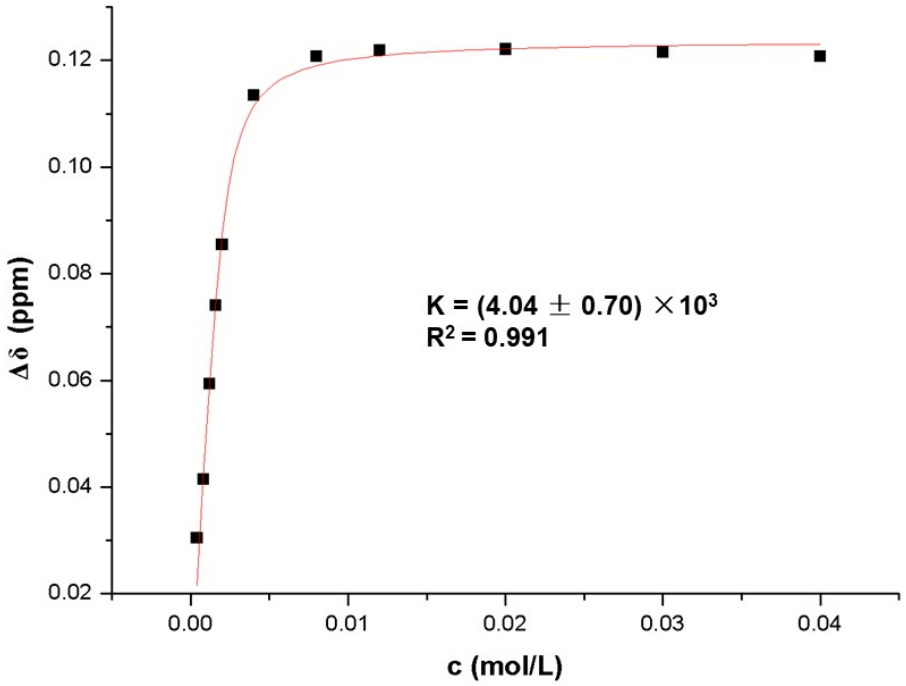

Fig. S33 The non-linear curve-fitting (NMR titrations) for the complexation of **2** (host) with 5' (guest) in CD_3CN at 298 K. Using the signal of **2** at δ 7.0761 as the reference. The association constant (*K*a) of **2⊃5'** in CD_3CN was estimated to be about (4.04 ± 0.70) ×10^3.

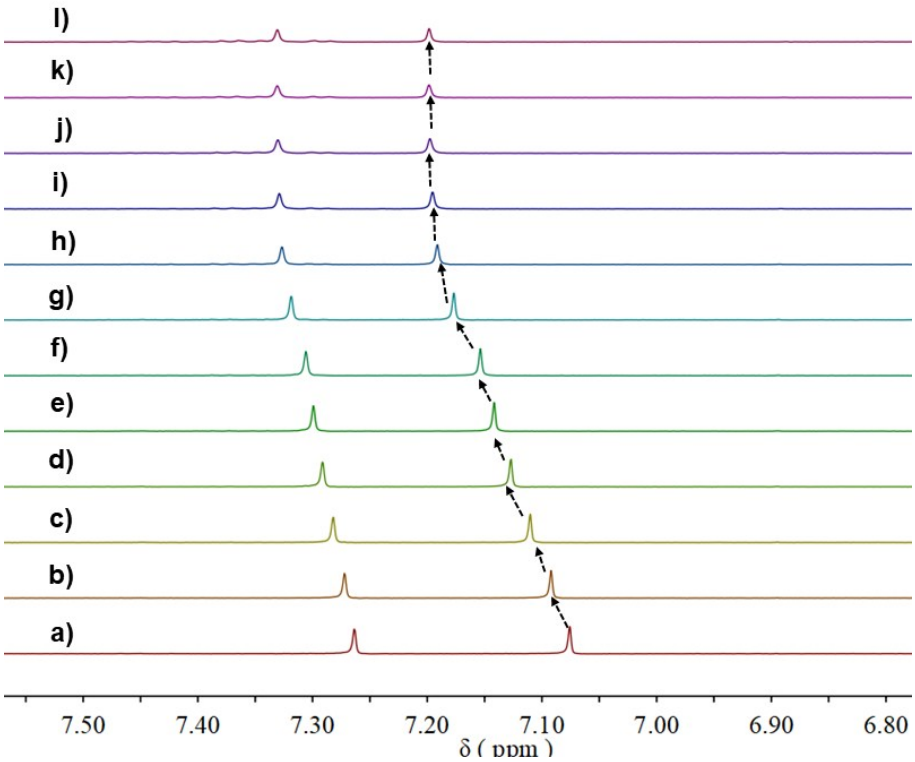

Fig. S34 Partial ^{1}H NMR spectrum changes (500 MHz, CD_3CN, 298 K) of **2** (host, 2.00 mM) upon addition of **6'** (guest): (a) 0.00, (b) 0.40, (c) 0.80, (d) 1.20, (e) 1.60, (f) 2.00, (g) 4.00, (h) 8.00, (i) 12.00, (j) 20.00, (k) 30.00, (l) 40.00 mM.

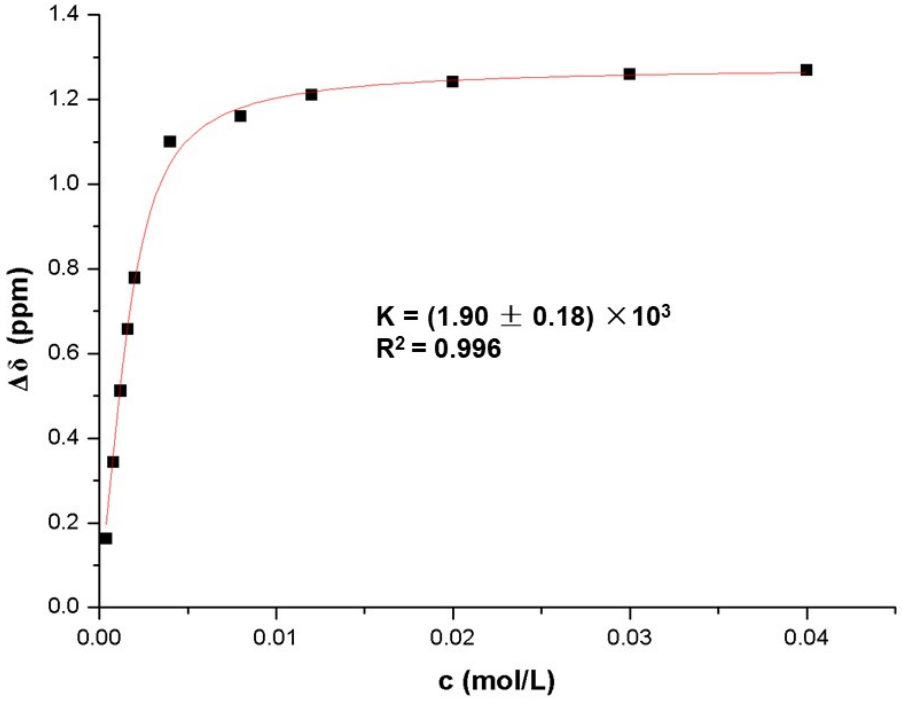

Fig. S35 The non-linear curve-fitting (NMR titrations) for the complexation of **2** (host) with **6'** (guest) in CD_3CN at 298 K. Using the signal of **2** at δ 7.0761 as the reference. The association constant (*K*a) of **2⊃6'** in CD_3CN was estimated to be about (1.90 ± 0.18) ×10^3.

4. Partial 2D NOESY NMR spectrum

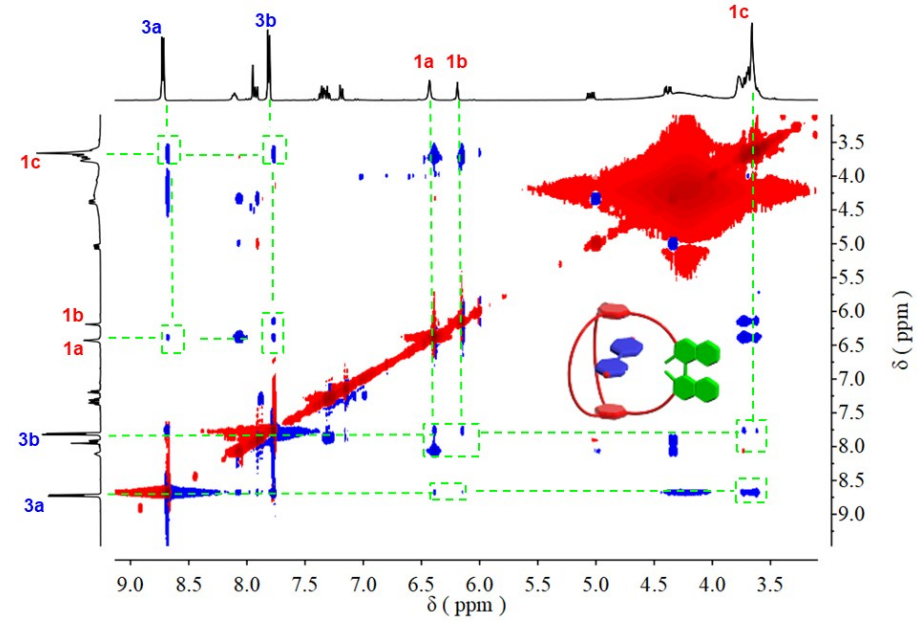

Fig. S36 Partial 2D NOESY spectra (400MHz, CD_3CN, 298 K) of **1⊃3'**

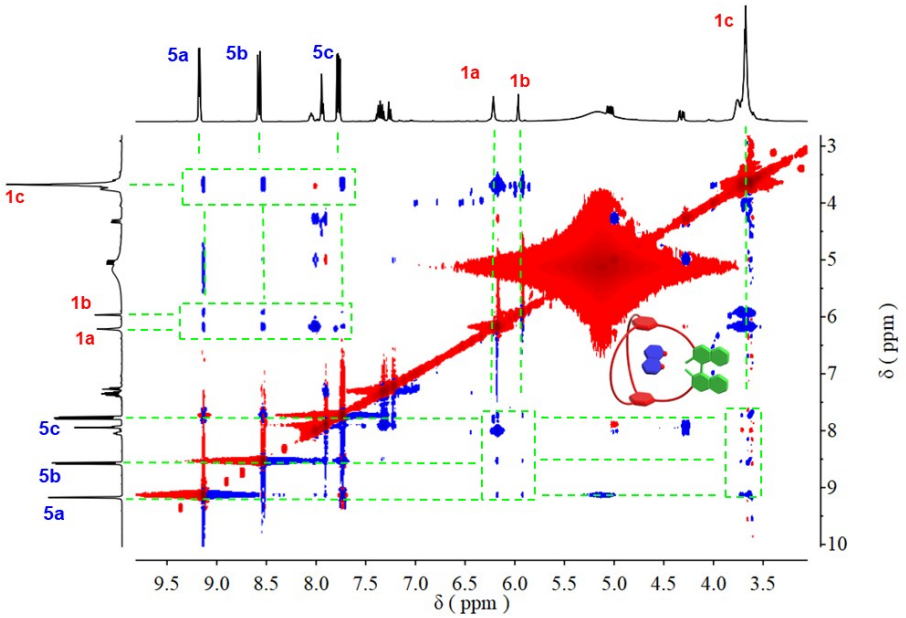

Fig. S37 Partial 2D NOESY spectra (400 MHz, CD_3CN, 298 K) of **1⊃5'**

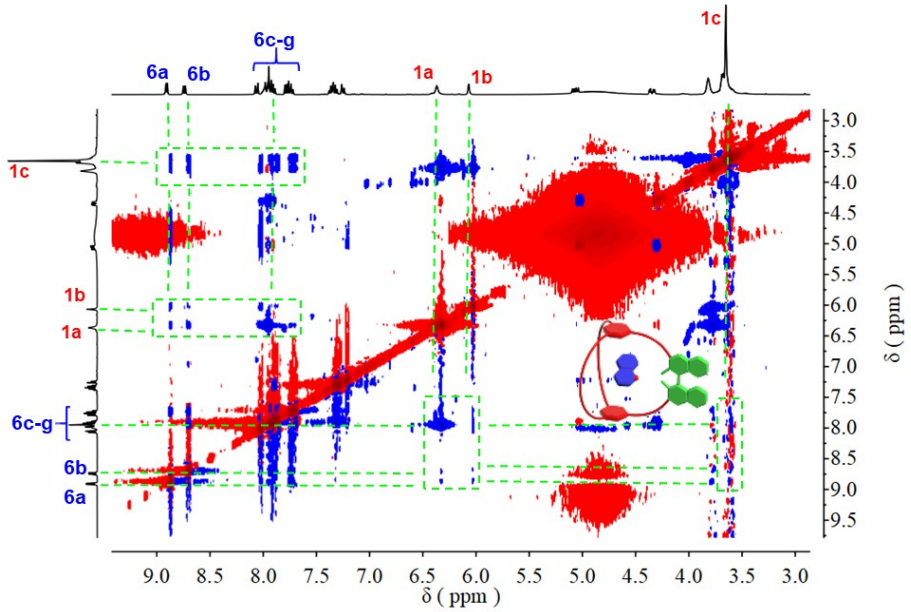

Fig. S38 Partial 2D NOESY spectra (400 MHz, CD_3CN, 298 K) of **1⊃6'**

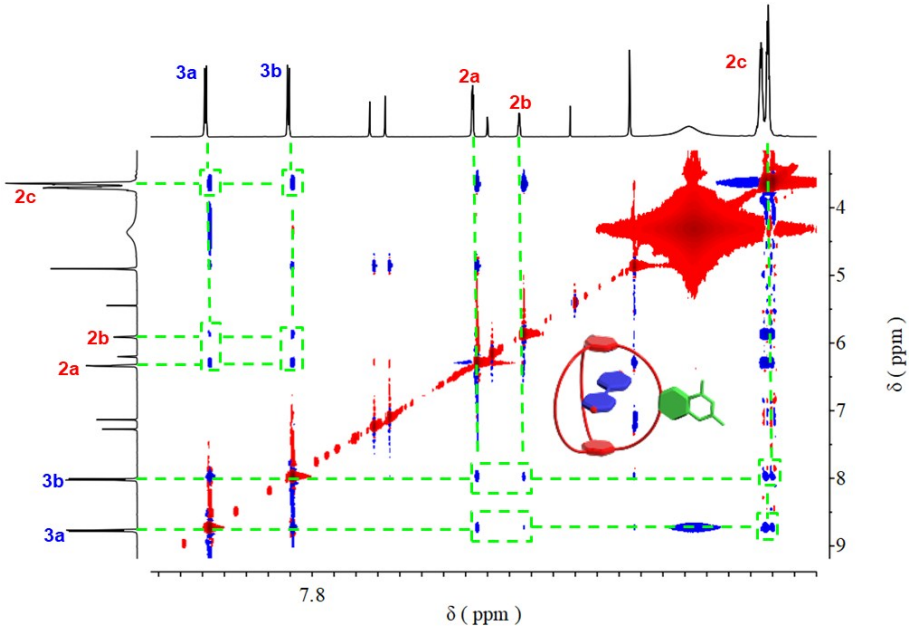

Fig. S39 Partial 2D NOESY spectra (400 MHz, CD_3CN, 298 K) of **2⊃3'**

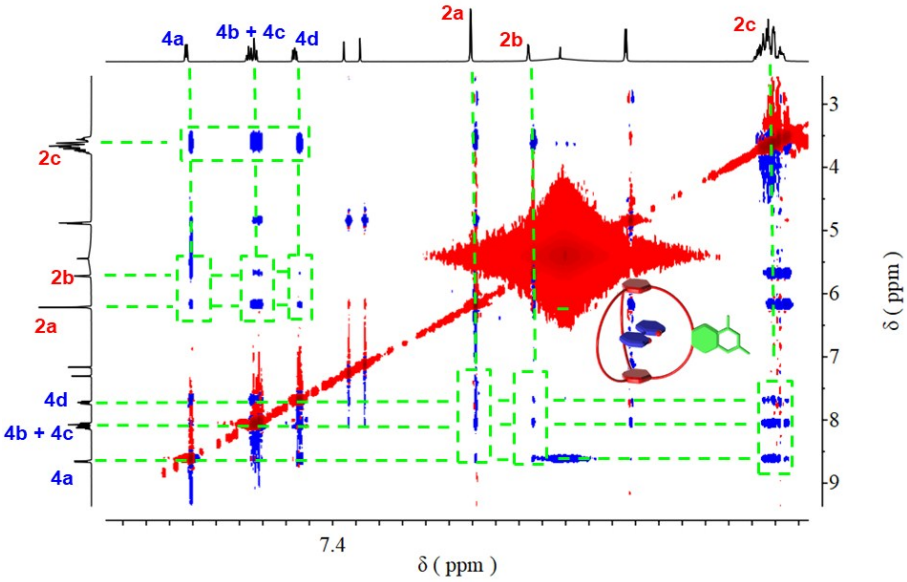

Fig. S40 Partial 2D NOESY spectra (400 MHz, CD_3CN, 298 K) of **2⊃4'**

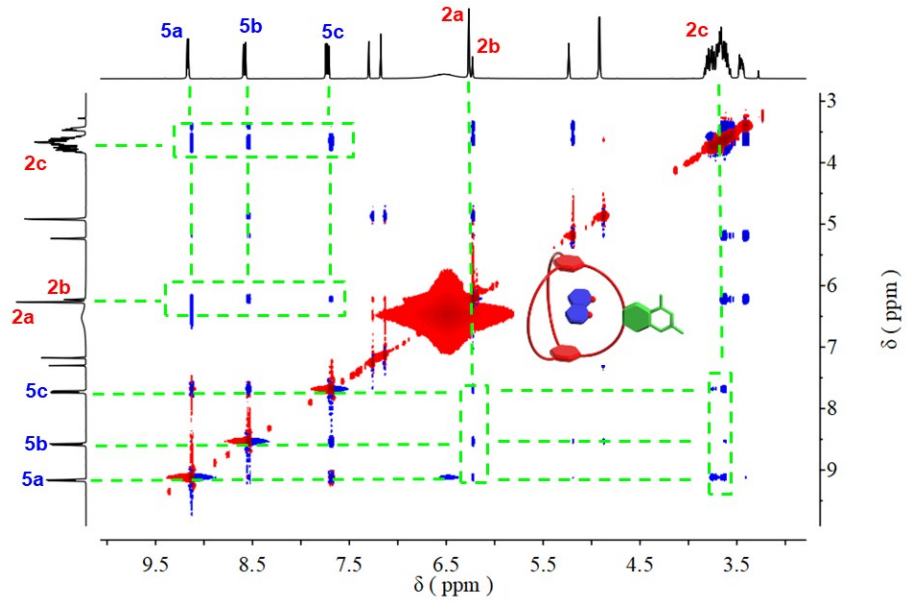

Fig. S41 Partial 2D NOESY spectra (400 MHz, CD_3CN, 298 K) of **2⊃5'**

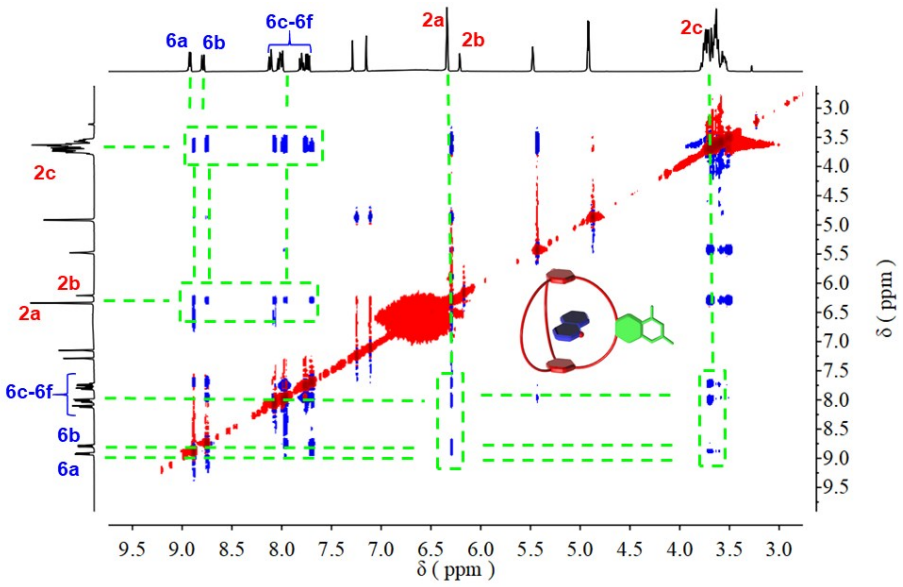

Fig. S42 Partial 2D NOESY spectra (400 MHz, CD_3CN, 298 K) of **2⊃6'**

5. X-ray crystal data for cryptand 1.

Table 1. Crystal data and structure refinement for **1**⊃paraquat.

CCDC number	1557481
Empirical formula	$C_{68}H_{75}F_{12}N_6O_{14}P_2$
Formula weight	1490.28
Temperature	296(2)
Wavelength	0.71073 Å
Crystal system	Orthorhombic
Space group	P 21 21 21
a	10.9020 (4) Å
b	17.44447(6) Å
c	38.6793(14) Å
α	90 °
β	90 °
γ	90 °
Volume	7356.1(5) $Å^3$
Z	4

Density (calculated)	1.346
Absorption coefficient	0.154
F(000)	3100
Crystal size	0.26 × 0.24 × 0.22 mm^3
Theta range for data collection	2.10 to 25.01 ^{o}
Index ranges	-12 <= h <= 12, -16 <= k <=20, -46<= l <=46
Reflections collected	54216
Independent reflections	12941 [R(int) = 0.0868]
Completeness to theta = 25.01°	99.8%
Absorption correction	\f and \w scan
Refinement method	Full-matrix least-squares on F^2
Goodness-of-fit on *F*2	1.106
Final R indices [$I > 2\sigma(I)$]	$R1 = 0.0868$, $wR2 = 0.2504$
R indices (all data)	$R1 = 0.0754$, $wR2 = 0.2337$
Largest diff. peak and hole	1.053 and -0.998 $e \cdot Å^{-3}$

6. References

1. H. Li, C.-S. Da, Y.-H. Xiao, X. Li and Y.-N. Su, *J. Org. Chem*, 2008, **73**, 7398-7401.
2. M. J. Gunter and M. R. Johnston, *Tetrahedron Lett.*, 1990, **31**, 4801-4804.